JOURNAL OF
POWER
SOURCES

A novel composite gel polymer electrolyte for rechargeable lithium batteries

Han-Hsin Kuo, Wei-Chih Chen, Ten-Chin Wen[*], A. Gopalan[1]

Department of Chemical Engineering, National Cheng Kung University, Tainan 701, Taiwan

Received 22 October 2001; received in revised form 18 March 2002; accepted 26 March 2002

Abstract

Composite polymer electrolyte (PE) films comprising of thermoplastic polyurethane (TPU) and polyacrylonitrile (PAN) (denoted as TPU–PAN) have been prepared by two different processes. Scanning electron microscope (SEM) of the films reveal the differences in morphology between them. The electrochemical properties of composite electrolyte films incorporating $LiClO_4$–propylene carbonate (PC) were studied. TPU–PAN based gel PE shows high ionic conductivity at room temperature. Thermogravimetric analysis informs that the composite electrolyte possesses good thermal stability with a decomposition temperature higher than 300 °C. Electrochemical stability in the working voltage range from 2.5 to 4.5 V was evident from cyclic voltammetry. Cycling performances of $Li/PE/LiCoO_2$ cells were also performed to test the suitability of the composite electrolyte in batteries. © 2002 Elsevier Science B.V. All rights reserved.

Keywords: Lithium battery; Thermoplastic polyurethane; Polyacrylonitrile; Composite polymer electrolyte

1. Introduction

Ionic conducting polymer electrolytes (PEs) which could be utilized for rechargeable lithium batteries have been widely investigated in the recent years [1–4]. Studies have been targeted as new polymer materials possessing high ionic conductivity, good mechanical properties and good thermal stability with an extrapolated utility in technological applications [5–8].

Ever since the discovery of poly(ethylene oxide) (PEO) electrolyte was launched by Wright [9], extended activities have been made on different solid state polymer electrolytes (SPE). In a solvent free PE system, it has been reported that conduction takes place predominantly in the amorphous phase, and the segmental mobility of the polymer chains determines the ionic mobility [10]. Unplasticized PEO electrolyte has low conductivity at ambient temperature due to the semicrystalline character and high glass transition temperature.

In order to improve the conductivity of the solvent free electrolytes, polymer is usually mixed with a polar solvent (plasticizer) such as ethylene carbonate (EC) or propylene carbonate (PC) [11]. This category of PE is called gelled polymer electrolyte (GPE) in which the liquid electrolyte solution has been immobilized by incorporating into a polymer matrix. In this case, the solvent plays the role of the ion supporting carrier and the plasticizer of polymer matrix, enhancing the mobility of ions and flexibility of PE. Besides PEO, polyacrylonitrile (PAN) [12,13], poly(vinylidene fluoride) (PVdF) [14,15] and poly(methyl methacrylate) (PMMA) [16,17] have also been used in making PEs. We have recently reported on the use of few of the thermoplastic polyurethane (TPU)-based electrolytes for battery applications [18–21].

Linear segmented polyurethane are $(A–B)_n$ type copolymers having alternating sequences of glassy or hard (A) material and rubbery or soft (B) material. The unfavorable interactions between the hard and soft segments make the system a microphase-separated one, which imparts elastomeric properties to polyurethane. The rubbery soft segments can dissolve alkali metal without formation of ionic cluster. On the other hand, the hard segment domains, which are in glassy state and are either distributed or interconnected throughout the rubbery phase, act as reinforcing filler and hence contribute to the dimensional stability the PEs. Because of this unique two-phase microstructure, the segmented polyurethanes find themselves very much useful as matrix materials for PEs. TPU doped with various alkali metal salts have been used as matrices for PEs [22,23].

It is known from several reports that use of PAN in electrolyte systems can impart several advantages. PAN systems show good mechanical strength as films and reported to be more thermally stable than PEO [24]. Besides these, dendrite growth in charging process of Li batteries can be inhibited by PAN. Hence, studies on the use of PAN in PE system are attractive. The PAN based PEs plasticized with liquid electrolyte can have relatively high ionic conductivity ($\sim 10^{-3}$ S/cm) at room temperature. However, these systems require a higher processing temperature [25].

In the present work, the composite electrolyte comprising of TPU and PAN was prepared. Morphology, thermal stability, electrochemical stability, ionic conductivity of the composite were investigated. A laminated cell was constructed to examine the rechargeable ability and to establish their use in practical application.

2. Experimental

2.1. Synthesis of thermoplastic polyurethane

TPU was synthesized in a batch reactor, comprising of four-necked round-bottomed flask with an anchor type stirrer, a nitrogen inlet, an outlet, and a thermocouple connected to a temperature controller. The soft segment, PTMG-2000 ($M_w = 2000$ g/mol, Aldrich), and the chain extender, 1,4-butanediol (1,4-BD, Aldrich) were kept in vacuum oven at 80 °C for 24 h to remove the moisture. First, 0.05 mol of soft segment and 0.20 mol of chain extender were put into the reactor, and then 0.25 mol of the hard segment, 4,4′-methylenebis(4-phenyl isocyanate) (MDI) was added stepwise. Dimethylformamide (DMF) was then used to control the viscosity of TPU during polymerization.

2.2. Molecular weight

The average molecular weight, M_n and M_w, of the PU prepolymer were determined by GPC (Shimadzu R-7A data module; LC-10AS pump). Two linear columns in series were used for separation. The flow rate for DMF was 2 ml/min at 40 °C using polystyrene standards. The weight-average molecular weight (M_w) was determined as 1.03×10^5 g/mol and for PDI as 2.04.

2.3. Preparation of the composite electrolytes

PAN (Polyscience, PA) of molecular weight 1.5×10^5 was dried under vacuum at 50 °C for 48 h. TPU and PAN powder were blended physically in the ratio of 1:1. The composite was dissolved in DMF and stirred vigorously for 1 h by using a homomixer. Then, solution casting was made to obtain a film on polypropylene plate. For obtaining the films, two drying processes were independently. In the first, the film was dried in vacuum oven at 50 °C. In the other process, drying was done by room temperature evaporation under vacuum. These films

were denoted as film A and film B, respectively. Both drying processes were sustained for 7 days. The films were then stored in an argon filled dry box (M. Braun GmbH, Germany). The thickness of the films were controlled between 80–100 μm.

2.4. Swelling study

Gel type electrolytes were prepared by dipping the dried composite films in 1 M LiClO$_4$–PC solutions at room temperature in a glove box. The percentage of swelling (S_w) was determined [18] by measuring the weight increase:

$$S_w = \frac{W - W_0}{W} \times 100\%$$

where W_0 is the weight of dried films and W is the weight of swelled films.

2.5. SEM

Micrographs of the composite films (A and B) were obtained using a JXA-840 scanning electron microscope (SEM) (JEOL, Japan). Photos were taken at vacuum after sputtering the sample with a thin gold film.

2.6. TGA

Thermal analysis of the composite film was made using a DuPont TA Instrument 2050 thermogravimetric analyzer under dry nitrogen atmosphere, with a heating rate of 40 °C/min and using platinum pans. The temperature range was from 25 to 800 °C.

2.7. Conductivity measurement

Impedance measurements were performed for thin films of the composites (46.5% TPU(PTMG)–PAN and 54.5% LiClO$_4$–PC) of about 100 μm in thickness and 0.785 cm^2 in area. The ionic conductivity of the composite films sandwiched between two stainless steel (SS) electrodes was obtained under an oscillation potential of 10 mV from 100 kHz to 0.1 Hz by using Autolab PGSTAT 30 equipment (Eco Chemie B.V., Netherlands) together with frequency response analysis (FRA) system software. Temperature of the cell was controlled using a thermostat (HAAKE D8 & G) and calibrated using a Pt resistance thermometer. The conductivity was calculated by

$$\sigma = \frac{1}{R_b} \times \frac{\lambda}{A}$$

where R_b is the bulk resistance from AC impedance, λ the film thickness, and A the surface area of electrode.

2.8. Cyclic voltammetry measurement

Cyclic voltammetry was performed using a three-electrode cell. The working electrode was SS (the type is stainless steel
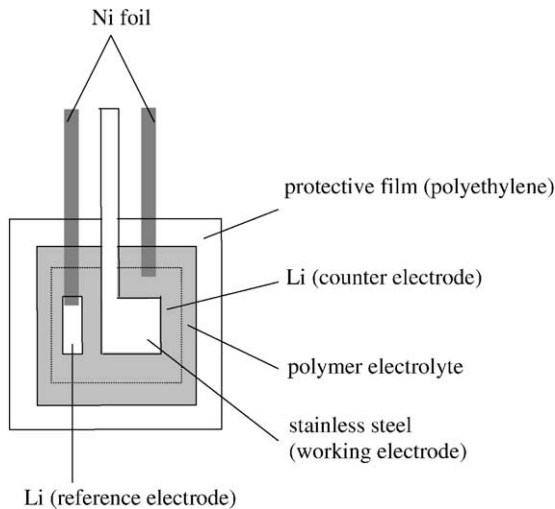
Fig. 1. Assembly of the cell used for cyclic voltammetry.

2.9. Assembly of laminated cell

Lithium metal and $LiCoO_2$ were employed as negative and positive electrodes, respectively. The area of both electrodes was fixed as 2.25 cm^2. $Li/PE/LiCoO_2$ laminated cells were assembled by pressing Li, PE, and $LiCoO_2$; sealed by polyethylene film, and laminated by an aluminum foil. Afterwards, the cells were cycled with BT-2043 system (Anbin electrochemical instrument, USA) between 4.2 and 2.7 V at room temperature.

3. Results and discussion

3.1. Morphology

304) with an area of 1 cm^2. Lithium metal was used for both the counter and reference electrodes. A cell was assembled as shown in Fig. 1. Measurements were performed on Autolab PGSTAT 30 electrochemical analyzer with general purpose electrochemical system software at room temperature.

The unplasticized composite films prepared from 1:1 PAN and TPU through drying at 50 °C (film A) and at room temperature (film B) exhibited different colors and appearance. Film B had an opaque appearance while the film A was a transparent one. In order to determine the morphological difference between these two films, SEM experiments were taken. Fig. 2 shows the SEM images of the two films of unplasticized 1:1 of TPU–PAN composites. It is clear to note
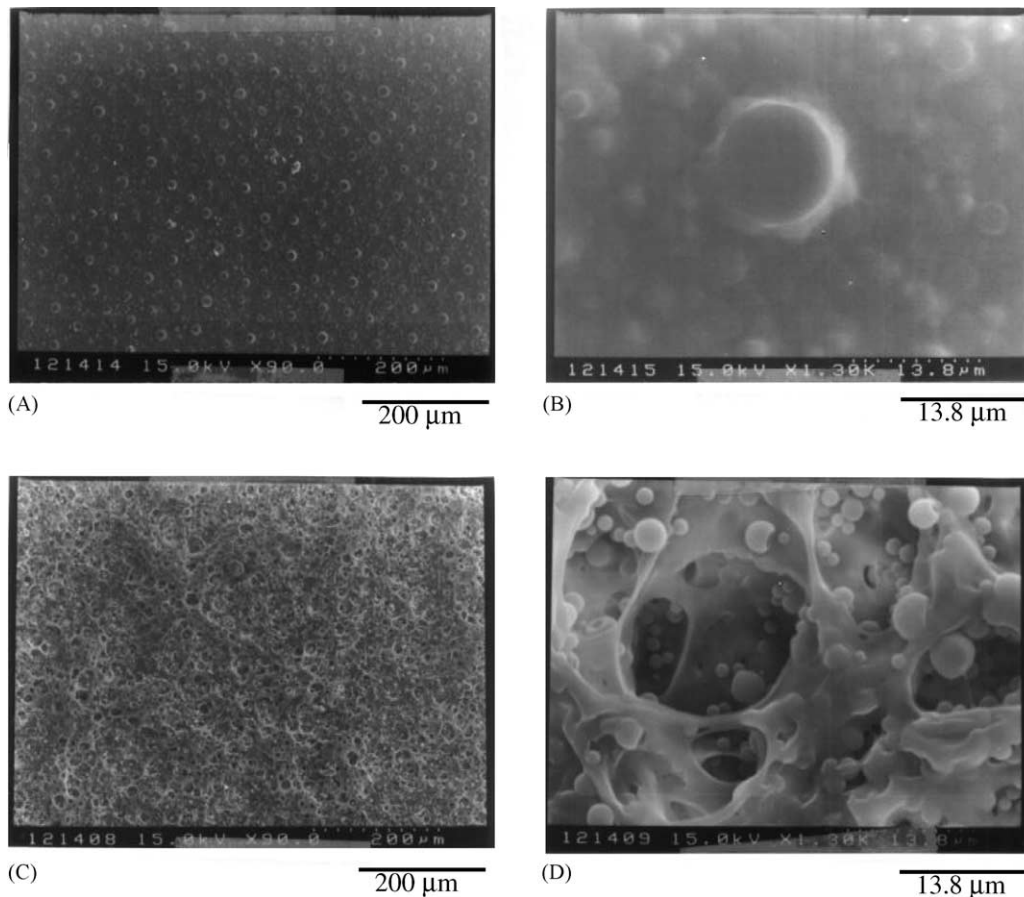

Fig. 2. The SEM photographs of TPU–PAN composites. (A) Film A (90×); (B) film A (1500×); (C) film B (90×); (D) film B (1500×). (Magnification is given in brackets).

from the SEM photograph that there are many pores in film B. On the other hand, film A is a compact and smooth one. It is to be noticed that the films were prepared by solution casting using DMF as solvent. The appearance of pores in film B is due to the preoccupation of moisture in the film. During the preparation of film B, the evaporation of DMF took place slowly and the content of DMF in the film decreases as evaporation proceeds. The hydrophilic groups in DMF traps H_2O molecules. When DMF content in the film became negligible, the entrapped H_2O molecules started evaporating out from the film leaving pores on the surface of the film. This resulted small pores in film B.

3.2. Arrhenius plot of conductivity

The composite films (A and B) were immersed in liquid electrolyte (1 M $LiClO_4$–PC). The content of liquid electrolyte in films A and B were estimated as 17.0 and 54.5%, respectively. In general, the conductivity of the PE increases with increasing the liquid electrolyte in the composite film [26]. Therefore, film A had lower conductivity than film B. The temperature dependency of the conductivity of the gel electrolyte film with 54.5% liquid electrolyte is presented in Fig. 3. The conductivity of PE obeys Arrhenius law. This implies that the conductive environment of Li^+ ions in the TPU–PAN composite is liquid like and remains unchanged in the investigated temperature region. The conductivity at 25 °C was calculated to be 1.0×10^{-4} S/cm. The activation energy (E_c) of as determined for this film by Arrhenius equation:

$$\sigma = \sigma_0 \exp\left(\frac{-E_c}{RT}\right)$$

where T is temperature on the Kelvin scale and σ_0 the proportional constant. E_c for TPU–PAN in the form of film
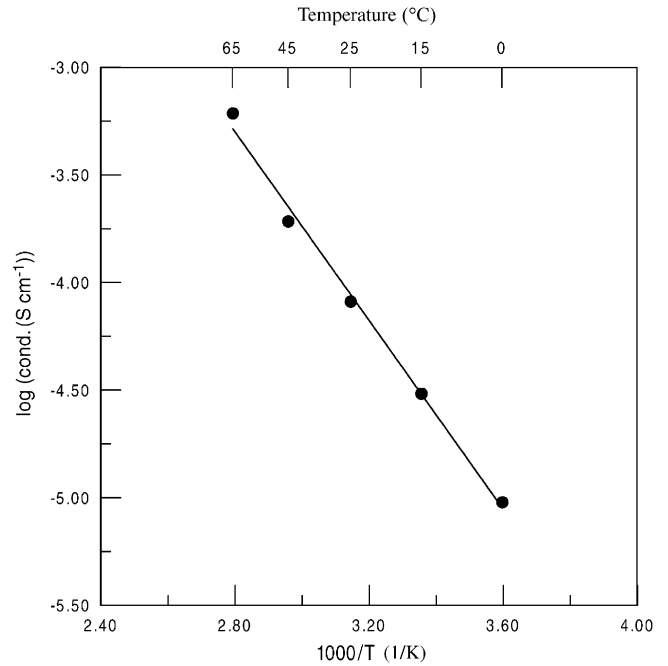
Fig. 3. Arrhenius plot of TPU–PAN composite (film B) containing 54.5% 1 M $LiClO_4$–PC.

B is 18.2 kJ/mol. This value is low in comparison with E_c values of TPU(PEG), TPU(PTMG), and PEO (29.3, 40.6, and 30.8 kJ/mol, respectively) [27], implying the better environment for ion conduction in this composite gel electrolyte.

3.3. Thermal analysis

Thermograms of TPU, TPU–PAN composite and PAN are shown in Fig. 4. TPU has a two-stage weight losses starting at about 296 °C with 5% residual mass at 450 °C. The parent
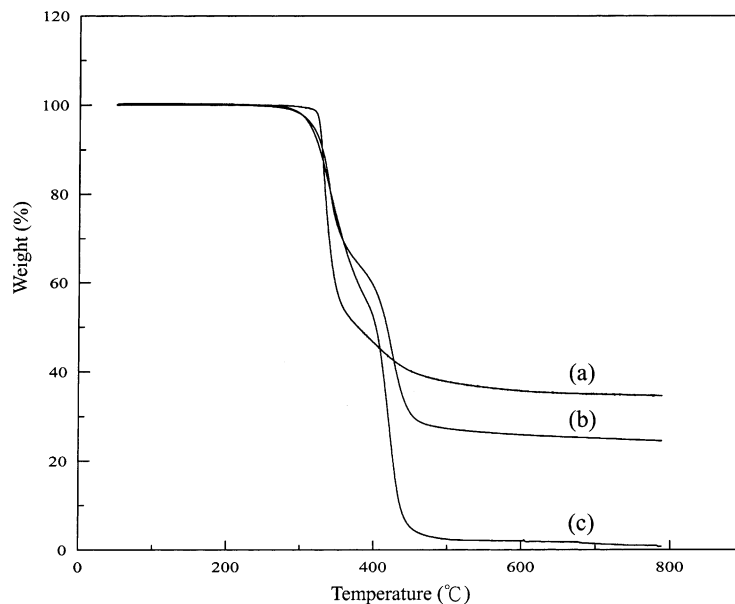
Fig. 4. TGA thermograms of (a) pure PAN; (b) TPU–PAN composite; (c) pure TPU.

PAN started losing weight at 319 °C with a drastic fall in weight thereafter. At 450 °C, PAN has 40% residual mass.

The decomposition of TPU–PAN composites followed a similar pattern in thermogram as that of pure TPU. The presence of PAN in the composite extends the decomposition temperature for the composites in comparison to pure TPU. The first weight loss of TPU–PAN composites was noticed at 309 °C. A residual weight of about 25% was present at 480 °C. Also, the composite showed a decomposition temperature (410 °C) for the second stage in comparison with TPU (400 °C). From these results, it may be concluded that the TPU–PAN composites have higher decomposition temperature than TPU film. Additionally, a decomposition temperature higher than 300 °C for TPU–PAN composite implies better thermal stability suitable for considering the composite PE in secondary lithium batteries.

3.4. Cyclic voltammetry studies

The cyclic voltammogram (CV) of the Li/PE/SS cell at room temperature is given in Fig. 5. The sweep rate was kept as 5 mV/s. The CV indicates a stable electrochemical potential window of 2.5–4.5 V versus Li/Li$^+$ on SS and hence, it can be taken that the stability window is at least 4.5 V for the composite electrolyte in our study. The CVs pattern of typical liquid LiClO$_4$–PC electrolytes and gel electrolytes are almost similar. This indicates that TPU–PAN composite has not affected the stability window of the electrolyte. The onset potential for Li deposition on SS was about −0.05 V and that can be taken as cathodic limit for the composite electrolyte. On sweeping the electrode potential, a cathodic peak was observed at around −0.32 V, which corresponds to the plating of lithium onto the SS electrode.

On the reverse scan, stripping of lithium was observed at around 0.39 V. The peak current tends to decrease with increase in cycle number and remains constant after few cycles. This phenomenon may be attributed to the formation of a passive layer on the SS electrode. As can be seen in Fig. 5, there are no more oxidation peaks up to 4.5 V (versus Li/Li$^+$). Thus, it is concluded that the TPU–PAN based PE has sufficient electrochemical stability to allow safe operation in rechargeable lithium battery systems. The reasons for this good electrochemical stability for TPU–PAN electrolyte can be viewed on line with other reports [12,28]. The addition of organic solvents and lithium salts to PAN based PE appears to influence the oxidation potential. Accordingly, the oxidative stability of organic esters (PC and EC) has been reported to be higher than that of ethers. PAN–LiClO$_4$ based electrolyte has higher electrochemical stability than any of the other PAN–lithium salt based electrolytes. Since LiClO$_4$ has higher lattice energy than the other known lithium salts that were employed electrolyte application, the interaction between the polymer and the lithium salt is considered to be relatively small and provides better electrochemical stability window.

3.5. Cycling performance

In order to investigate the utility of the TPU–PAN based PE in making a cell assembly with an anode and a cathode in a lithium ion polymer battery, a Li/PE (TPU–PAN)/LiCoO$_2$ cell was constructed. The theoretical capacity of the LiCoO$_2$ electrode was found to be 120 mAh/g. Cycling tests were performed at the C/20 cycling rate and with cut-off voltages as 4.2 and 2.7 V for the upper and lower limits, respectively. The cut-off voltage was so selected to prevent destroying of
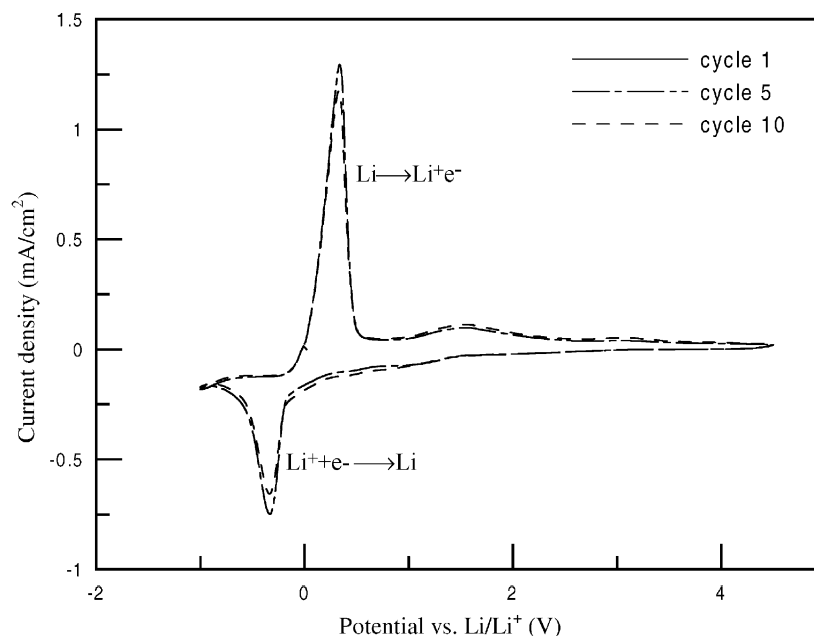

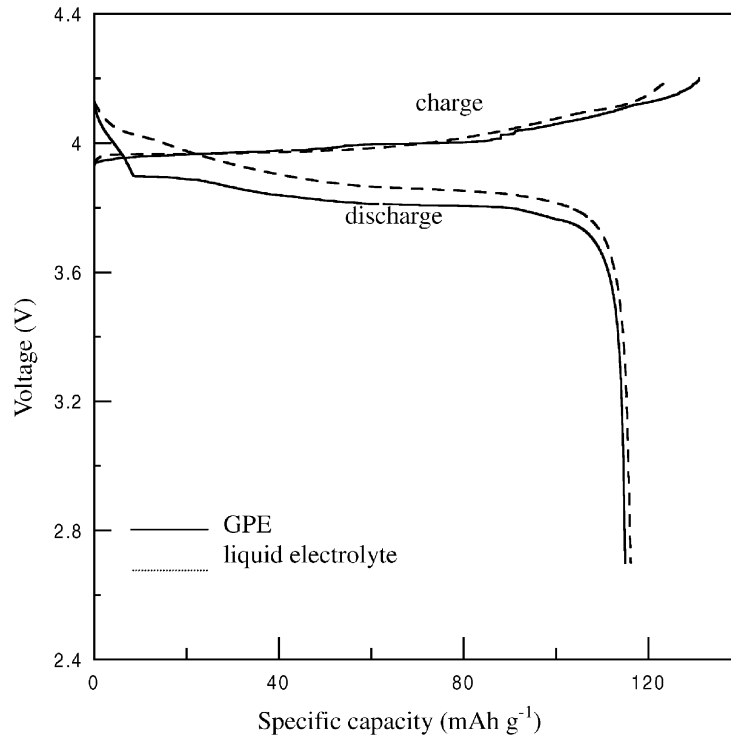Fig. 5. CV of Li/PE (TPU–PAN)/SS cell. Sweep rate = 5 mV/s.

Fig. 6. The third cycle charge–discharge performance of Li/PE (TPU–PAN)/LiCoO$_2$ and Li/1 M LiClO$_4$–PC/LiCoO$_2$ cells.

the crystallinity of LiCoO$_2$. In the charge reaction, the x in Li$_x$CoO$_2$ gradually decreases from 1 to 0.55. For values of x lower than 0.55, the oxidation of Co^{3+} to Co^{4+} becomes possible [29,30]. This may alter crystallinity of the cathode and cause decrease in reversibility. Therefore, the depth of discharge was restricted to <120 mAh/g of LiCoO$_2$ to have high cycling performances.

To assess and compare the performance of TPU–PAN composite PE, a simple cell with 1 M LiClO$_4$–PC was used as liquid electrolyte. The charge–discharge curves of Li/TPU–PAN/LiCoO$_2$ and Li/LiClO$_4$–PC/LiCoO$_2$ cells at the third potential cycle are given in Fig. 6. It is obvious that the cell at C/20 rate achieves a capacity of 114.9 mAh/g. A comparison among the discharge curves reveals that the
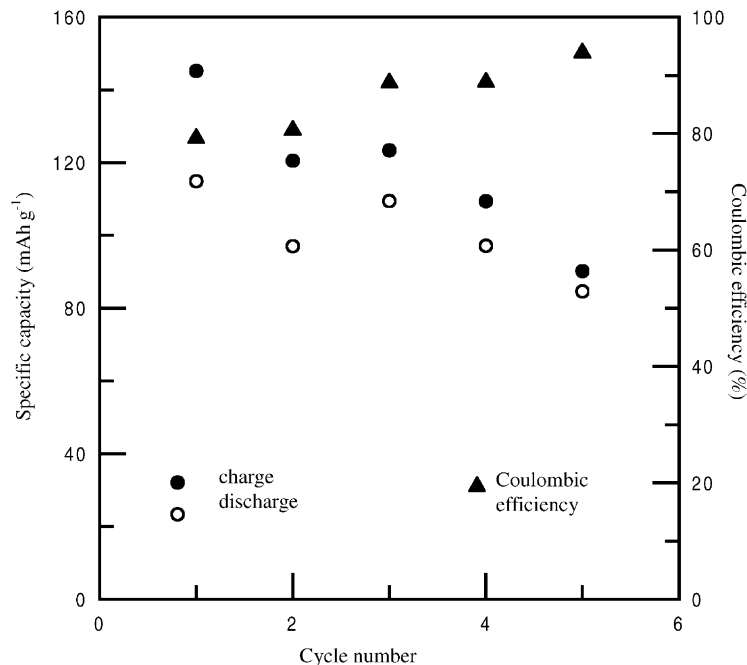

Fig. 7. Charge–discharge capacity and coulombic efficiency of a Li/PE (TPU–PAN)/LiCoO$_2$ cell as a function of cycle number at C/20 rate.

capacity of PE is slightly lower than that of liquid electrolyte (Fig. 6). The reduced capacity is attributed to the lower diffusion rate of lithium ions in the PEs as compared with that in liquid electrolyte.

The charge–discharge capacities and coulombic efficiency of the Li/PE/LiCoO$_2$ cell as a function of cycle number are presented in Fig. 7. The charge capacity of the cell decreases as the cycle number increases, and after five cycles, the capacity was only about 70% of the theoretical capacity. The coulombic efficiency was estimated to be more than 90% after initial three cycles. The phenomenon that the large irreversible capacity observed in the first cycle can be ascribed to an initial poor interfacial contact between the PE and Li electrode. This necessitates activation of Li/PE interface by using initial flow of current. Upon cycling further, the decrease in capacity may be due to the formation of a passive layer on the surface of the lithium electrode, resulting from PC [8,31]. However, the passive layer is continuously formed during cycling [4], and behaves as an electronically insulating film which protected it from further attack [31]. Hence, the passive layer makes difficulty in charge transfer in lithium electrode and the diffusion rate of Li$^+$ ion in the Li/PE interface becomes very slow [7,18]. Accordingly, the loss of capacity on cycling was caused by the increasing of interfacial resistance which resulted from the degradation of Li/PE interface. It is known that lithium can be plated with high efficiency and could result problems in making practical rechargeable cells with lithium metal as negative electrode. The high reactivity of the newly plated lithium with components of the electrolyte could make undesired passive layers. Therefore, a part of the lithium grains may be lost due to electronic isolation from the rest of the electrode and thus causes decrease in capacity.

4. Conclusion

The morphology, conductivity and thermal stability were established for a new type of porous PE composed of TPU and PAN. The preparation of the TPU–PAN gel PE seems to be more convenient than the traditional way of making PAN based electrolyte. The TPU–PAN composite possesses good mechanical properties. The TPU–PAN based gel PE displays high conductivity at room temperature. The existence of PAN in the composite improved the thermal stability. The lithium plating-stripping process is a reversible and implies better electrochemical stability in the working voltage range. The Li/PE (TPU–PAN)/LiCoO$_2$ cell was successfully constructed and the performance was assessed. The formation of passive layer at Li/PE interface influences the charge–discharge characteristics. In general, the TPU–PAN composite is known to have the advantage of ease of preparation,

thermal stability and conductivity than simple PAN based electrolyte.

Acknowledgements

References

[1] H.V. Venkatasetty, J. Power Sources 97/98 (2001) 671.
[2] F.R. Kalhammer, Solid State Ionics 135 (2000) 315.
[3] Y.G. Andreev, P.G. Bruce, Electrochim. Acta 45 (2000) 1417.
[4] G.B. Appetecchi, F. Alessandrini, R.G. Duan, A. Arzu, S. Passerini, J. Power Sources 101 (2001) 42.
[5] D. Fauteux, A. Massucco, M. Mclin, M. van Buren, J. Shi, Electrochim. Acta 40 (1995) 2185.
[6] D.W. Kim, J. Power Sources 76 (1998) 175.
[7] H.S. Kim, B.W. Cho, J.T. Kim, K.S. Yun, H.S. Chun, J. Power Sources 62 (1996) 21.
[8] S. Slane, M. Salomon, J. Power Sources 55 (1995) 7.
[9] D.E. Fenton, J.M. Parker, P.V. Wright, Polymer 14 (1973) 589.
[10] A. Magistris, K. Singh, Polym. Int. 28 (1992) 277.
[11] R. Huq, R. Koksbang, P.E. Toner, G.C. Farrington, Electrochim. Acta 37 (1992) 1681.
[12] F. Croce, F. Gerace, G. Dautzemberg, S. Passerini, G.B. Appetecchi, B. Scrosati, Electrochim. Acta 39 (1994) 2187.
[13] D. Peramunage, D.M. Pasquariello, K.M. Abraham, J. Electrochem. Soc. 142 (1995) 1789.
[14] H.S. Choe, J. Giaccai, M. Alamgir, K.M. Abraham, Electrochim. Acta 40 (1995) 2289.
[15] J.M. Tarascon, A.S. Gozdz, C.N. Schmutz, F. Shokoohi, P.C. Warren, Solid State Ionics 86–88 (1996) 49.
[16] G.B. Appetecchi, F. Croce, B. Scrosati, Electrochim. Acta 40 (1995) 991.
[17] X. Liu, T. Osaka, J. Electrochem. Soc. 144 (1997) 3066.
[18] T.C. Wen, W.C. Chen, J. Power Sources 92 (2001) 139.
[19] T.C. Wen, H.H. Kuo, A. Gopalan, Macromolecules 34 (2001) 2958.
[20] H.L. Wang, H.M. Kao, M. Digar, T.C. Wen, Macromolecules 34 (2001) 529.
[21] H.L. Wang, H.M. Kao, T.C. Wen, Macromolecules 33 (2000) 6910.
[22] M. Seki, K. Sato, R. Yosomiya, Makromol. Chem. Macro. Chem. Phys. 193 (1992) 2971.
[23] J.D. Vanheumen, J.R. Stevens, Macromolecules 28 (1995) 4268.
[24] H. Huang, L.Q. Chen, X.J. Huang, R.J. Xue, Electrochim. Acta 31 (1992) 1671.
[25] K.M. Abraham, H.S. Choe, D.M. Pasquariello, Electrochim. Acta 43 (1998) 2399.
[26] D.W. Kim, Y.R. Kim, J.K. Park, S.I. Moon, Solid State Ionics 106 (1998) 329.
[27] T.C. Wen, W.C. Chen, J. Appl. Polym. Sci. 77 (2000) 680.
[28] J.M. Tarascon, D. Guyomard, Solid State Inoics 69 (1994) 293.
[29] J.N. Reimers, J.R. Dahn, J. Electrochem. Soc. 139 (1992) 2091.
[30] J. Kleinberg, W.J. Argersinger, E. Griswold, Inorganic Chemistry, D.C. Heath and Co., Boston, 1960, pp. 550–551.
[31] A.N. Dey, B.P. Sullivan, J. Electrochem. Soc. 117 (1970) 222.